INTERNATIONAL JOURNAL
FOR RESEARCH

IN APPLIED SCIENCE & ENGINEERING TECHNOLOGY

Computer-Aided Detection of Bone Metastasis using Bone Scintigraphy Scans

Saumya Srivastava[1], Omika[2], Shatakshi Pandey[3], Sanjay Maurya[4]

[1, 2, 3, 4]*Department of Electronics & Communication Engineering, Shri Ramswaroop Memorial College of Engineering and Management, Lucknow, India*

Abstract: When cancer cells spread from their original site to the bone then it is known as 'Bone Metastasis'. Patients with solid tumors such as lung, breast, kidney, prostate etc. oftentimes develop bone metastasis. Cancer cells that spread to the bone mostly affect limbs, pelvis, spine, skull and ribs. Once tumors have metastasized to the bone, patients usually undergo skeletal complications collectively known as skeletal-related events (SRE) like skeletal remodelling, fractures, spinal cord compression, pain or anaemia and bowel incontinence. Therefore, early diagnosis of bone metastasis is crucial for increasing survivability as it has a major impact on treatment decision and at the same time it is a decisive factor in the evolution of the disease and the quality of life. 'Bone Scintigraphy' is accepted to be an efficient diagnostic tool for whole-body examination of bone metastasis. Computer-Aided Detection method is used to avoid mistakes which might be caused by human interference & experimental sources. CAD system provides faster and more precise results that facilitates in the early detection of bone metastasis, hence increasing the patient's chance of survival. To reduce the dependency of the system on source of the input image & for making the system robust we have explored various done image enhancement techniques.
Index Terms: WBS, CNN, GC, CAD, DNN.

I. INTRODUCTION

Cancer refers to the disease which involves uncontrollable growth of cells present in the body and its spread to the other parts of the body. It can originate in any part of the body. Old and damaged cells die & get replaced by new cells. If this orderly process breaks down, then it results into abnormal or damaged cell growth and their multiplication. These cells give rise to tumors i.e., lumps of tissue. Tumors can be categorized into two types : cancerous (malignant) or non-cancerous (benign). Benign tumors do not spread whereas malignant tumors invade nearby tissues and form new tumors which is commonly termed as metastasis.

When cancer cells break away from their original site passing through the blood or lymph system, and forms a new tumour in other organs or tissues of the body then it is known as 'Metastasis'. And when these cancer cells spread from their primary location to the bone then it is termed as 'Bone Metastasis'. Metastasis is one of the main reasons causing death of cancer patients. Approximately 3–10% of breast cancer patients have metastatic disease which represents a high rate. Patients with solid tumors such as lung, breast, kidney, prostate etc. oftentimes develop bone metastasis. Whole-body Bone Scan (WBS) or Bone scintigraphy Scan is extensively accepted as a standard method for surveying the presence and level or stage of bone metastasis since it is much cheaper than MRI and has similar performance. An automated bone metastasis detection model based upon multi-view images is proposed. This model aims to extract, aggregate, and classify high-level features in a data-driven manner. A feature aggregation operator parameterized by a deep neural network is proposed for binding the features of anterior and posterior views of an examination.

Bone Scintigraphy or Bone Scan Images are used for determining the hotspots. It is a special type of nuclear medicine procedure which uses small amount of radioactive material to diagnose and assess the severity of a variety of bone diseases including cancer of the bone or metastasis. The skeletal scintigraphy images are further enhanced by improving the dark parts present in the bones to help the specialists in interpreting the diagnostic radiology easily. Automated bone scan analysis ensures reliability and efficiency of bone metastasis diagnosis.

II. PRE- PROCESSING

The objectives of this project are divided into four different modules which are enumerated below.

The bone scintigraphy scan images collected were obtained from publicly available and general dataset consisting of 82544 bone scan images associated with 3247 patients from West China Hospital, named BS-80K. All images in BS-80K were de-identified to protect patients' privacy. 6176 images were having a resolution of 256×1024 pixels and 9298 images were having a resolution of 512×1024 pixels. For scans of non-metastasis patients IEEE dataset was used which consisted 37 bone scan images having resolution of 128×512.
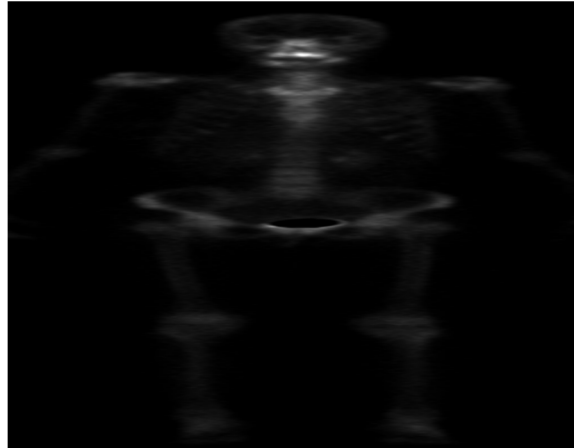
Fig. 1 Input Bone Scintigraphy Scan Image.

In the original WBS image the bone area is white in colour with a black but the colour is reversed in order to improve the presentation. Negative imaging of WBS images is done producing images with white background and black bone area. It not only improves the presentation of the image but also makes it easier to notice hotspot which is the determining factor of bone metastasis.

Fig. 2 Negative Image of Bone Scintigraphy Scan.

III.   IMAGE ENHANCEMENT & OPTIMIZATION

Enhancement is done to increase the contrast of the image which helps in interpreting more information from any image which cannot be seen in normal images. Gamma Correction (GC) in which power law equation is used to brighten up the low intensity areas of dark bone scan images, without any loss in clinically significant details. It is feasible with single gamma value of 0.5 and range of 0.4–0.7 gave best results. The Effective Measure of Enhancement (EME) score of processed images numerically indicated that the brightness of the processed image was visually improved but still there was little deviation from the mean intensity of input image which avoided a washout appearance.

Fig. 3 Gamma Corrected Image.

IV.   SEGMENTATION OF REGION OF INTEREST (ROI)

The enhanced images are subjected to segmentation to extract the hotspot region from the bone scan images which are essential in detection of bone metastasis. In this project, the segmentation process is carried out using Canny Edge Detection & Morphological Closing.

Before segmentation, the intensity values of the image is adjusted using imadjust function by specifying the range of intensity values in the output image. It saturates the bottom 1% & top 1% of all pixel values. It increases the contrast of output image.

Fig. 4 Adjusted Image.

For any image, an edge is curve which follows a path of rapid change in image intensity. Edges are mostly associated with the boundaries of objects in a scene. Edge detection identifies the edges in the image. Canny method is considered to be the most powerful edge-detection method that provides edge. Canny method is different from the other edge-detection methods as it uses two different thresholds to detect strong and weak edges, including the weak edges in the output only if they are connected to strong edges.

Fig. 5 Edge Detected Image.

Morphological closing is an operation present in mathematical morphology that is commonly used in image processing and computer vision. It is a process that involves two steps: Dilation and Erosion. The dilation operation involves expanding the boundaries of an object present in an image, by replacing each pixel with the maximum intensity value in its local neighborhood. This process helps to fill in gaps and holes present in the object, making it complete and more connected.

The erosion operation involves shrinking the boundaries of an object, by replacing each pixel with the minimum intensity value present in its local neighborhood. This process helps to remove small isolated pixels which may not belong to that object.

Morphological closing combines these two operations by first performing a dilation operation on the given image, followed by an erosion operation on the result. The purpose of this operation is to eliminate small holes and gaps in an object while preserving its shape and size.

By applying morphological closing to the image, we remove small gaps and holes in the object, which help to improve the accuracy of subsequent segmentation algorithms.

Fig. 6 Closed Edges Image.

There are still some gaps or holes present after applying edge closing as we can see in Fig. 6. Those holes are filled using imfill function to give Fig. 7.

Fig. 7 Filled Edges Image.

V. FEATURE EXTRACTION

Feature extraction refers to extraction of a vector based on different properties of the image. The feature vector serves as an input to the classifier for its purpose of classification.

GLCM features show us the information for the texture of the image. GLCM (Gray-Level Co-occurrence Matrix) is a matrix which describes the second-order statistics of an image. It represents how often pairs of pixels with specific values and spatial relationship occur in the image. GLCM features are statistical measures extracted from the GLCM matrix. These features are used to describe the texture properties of the image. Some commonly used GLCM features are shown in TABLE I.

TABLE I

FEATURES	DESCRIPTION	FORMULAE.
Correlation	It is likeness between a reference point in the image to the image itself.	$\sum_{i,j} \dfrac{(i-\mu)(j-\mu)p(i,j)}{\sigma_\tau \sigma_j}$
Energy	The rate of change in any feature like brightness is called energy.	$\sum_{i=j} p(i,f)^2$
Homogeneity	It refers to the property which shows similarity between each pixel color.	$\sum_{i,j} \dfrac{p(i,j)}{1+|i-j|}$
Contrast	It is the measure of intensity variation of an image in GLCM matrix.	$\sum_i |i-j|^2 p(t,j)$

Convolutional Neural Network (CNN) is also explored to automatically extract high level features from the input images. CNN has shown great success in computer vision field, due to its powerful feature extraction abilities. The operation in the convolution layer can be formulated as follows :

$$\begin{cases} z_{i,j}^{l+1} = \sum_{p=0}^{P_1-1} \sum_{q=0}^{Q_l-1} \sum_{k=0}^{K_l-1} w_{p,q,k}^l \cdot a_{i+p,j+q,k}^l \\ a_{i,j}^{l+1} = f\left(z_{i,j}^{l+1}\right) \end{cases} \tag{1}$$

Where $w_{p,q,k}^l$ are parameters of convolution filter in lth convolutional layer, *P, Q* and *K* denote the width, height and channel of the filter. *i* & *j* define the spatial location of one element in feature map z^{l+1}, *f* is non-linear activation function, which is a rectified linear unit (ReLU) function.

VI. CLASSIFICATION

Classification in image processing is a technique which is used for detecting diseases from medical images such as X-rays, MRI scans, CT scans, ultrasound images, and Scintigraphy scans. This technique involves training a machine learning algorithm on a dataset of images which are labelled with the presence or absence of bone metastasis. The algorithm then uses the learned features to classify new images into either having the metastasis or not. Training a CNN involves providing a large set of labelled images to the network, and adjusting the weights of the layers to minimize the difference between the predicted outputs and the true labels. Once trained, a CNN can be used to classify new images or extract high-level features that can be used for other tasks such as object detection, image segmentation, and content-based image retrieval.

AlexNet is popular CNN architecture that has been used for image classification tasks. It is 8 layers deep. The network is composed of multiple convolutional and pooling layers that learn the features of the input images. Architecture of AlexNet is shown in Fig. 8. The features learned by the CNN can then be used for classification tasks. Performance evaluation of this model is done using Sensitivity, Specificity, Accuracy, and F1-score as evaluation criteria. These parameters are formulated in TABLE II.
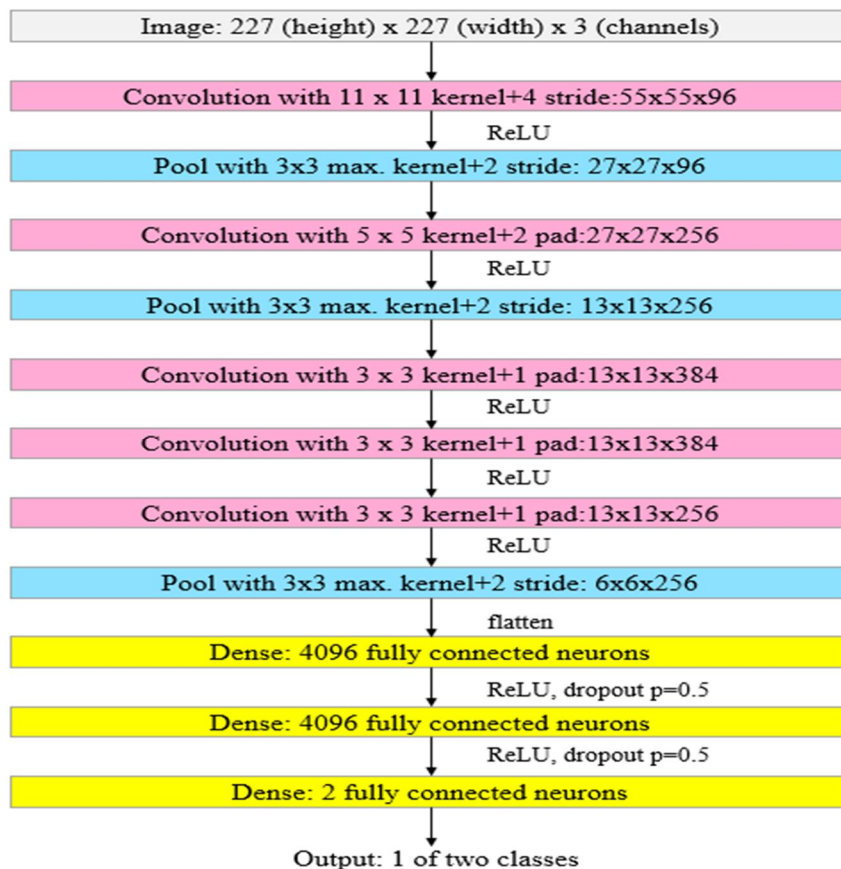
Fig. 8 Architecture of AlexNet

TABLE II

Parameters	Formulae
Sensitivity	$\dfrac{TP}{FN + TP}$
Specificity	$\dfrac{TN}{FP + TN}$
Accuracy	$\dfrac{TP + TN}{TP + TN + FP + FN}$
Precision	$\dfrac{TP}{TP + FP}$
Recall	$\dfrac{TP}{TP + FN}$
F1-score	$2 * \dfrac{Precision * Recall}{Precision + Recall}$

Where TP refers to True Positive, TN refers to True Negative, FP refers to False Positive and FN refers to False Negative.
Various modules involved in this project for detection of bone metastasis are manifested in the block diagram for the proposed methodology shown in Fig. 9.
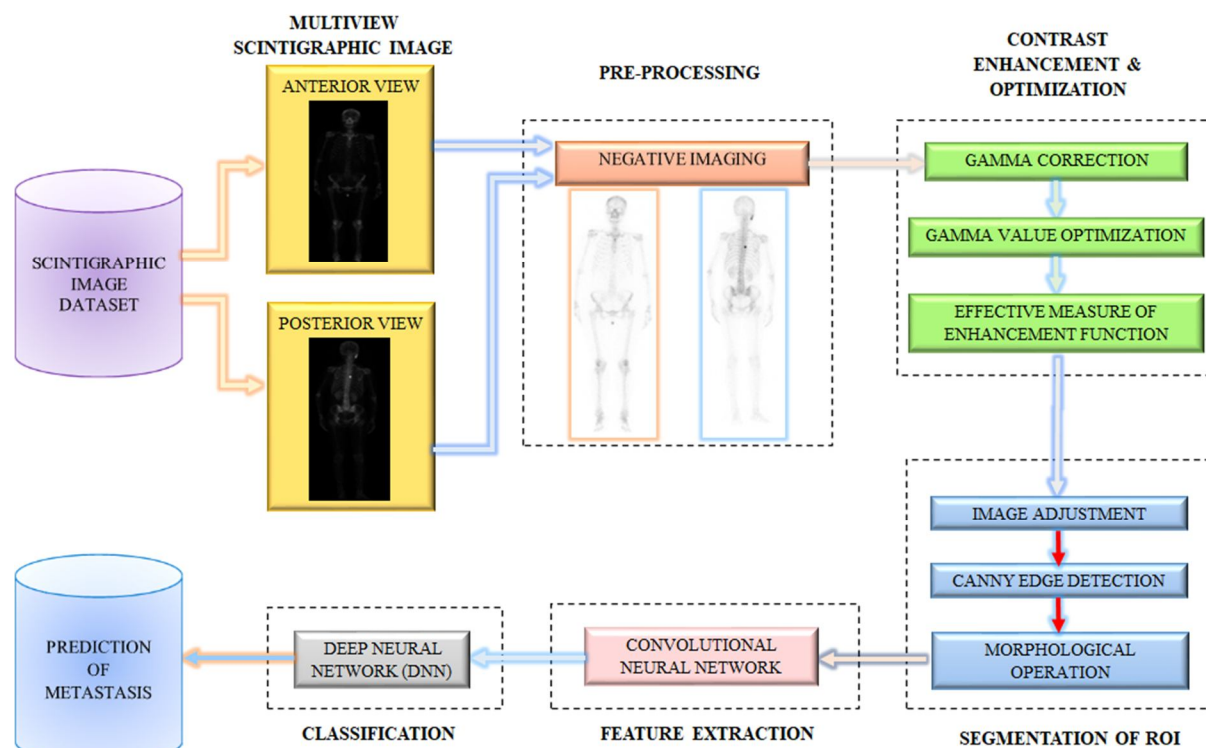
VII.   BLOCK DIAGRAM

Fig. 9 Block Diagram of Computer- Aided Detection of Bone Metastasis using Bone Scintigraphy Scans.

VIII.   REVIEW OF PREVIOUS WORKS

Application of Computer-Aided Detection systems (CAD) to WBS images has been a subject of study for decades. This section gives an overview of previous studies related to each module of the proposed methodology:

F.G. Elfarra et al. [1] have proposed an adaptive filtering technique based on Kuwahara Filter to suppress the noise in bone scintigraphy images. This filter applies smoothing on the image while preserving the position & magnitude of edges. It introduced Parallelepiped Classification (PC) method for generating the radionuclide distribution map for detection of bone metastasis. It automatically categorizes all pixels in bone scintigraphy images in individual classes based on pixel values to generate bone classification map. However, validation of the method on a larger group of patients is required.

M. M. Nasef et al. [2] have proposed a technique that enhances the dark regions of the skeletal scintigraphy images. The optimization problem is solved using the Neutrosophic domain and Salp Swarm algorithm (SSA). This paper shows that it can depend on falsity membership of Neutrosophic set in the field of Image Enhancement.

M.A. Calin et al. [3] used median filter to address noise issue in whole-body bone scintigraphy images to improve image quality. It reduces noise in the image by replacing each pixel value with neighbouring pixels' median value**.** But sometimes this filter reduces the edge information while denoising process. It detects and classifies bone metastasis using K-Nearest Neighbour (KNN) and gives the accuracy of 86.62% or Support Vector Machine (SVM) which gives the accuracy of 86.81%. Segmentation input parameters significantly affected the classification performance of the Object-Oriented Classification (OOC) method.

A. Sharma et al. [4] proposed algorithm based on the Gamma Correction (GC) in which power law equation is used to brighten up the low intensity areas of dark bone scan images, without any loss in clinically significant details.

A. Aslantas et al. [5] proposed a Level Set Active Contour (LSAC) segmentation algorithm was used to segment homogeneous images by their intensity. It shows a high detection rate, with 94% sensitivity and 86.67% specificity. However, a larger database would have improved the accuracy of the results. They proposed a novel image gridding method for feature extraction of metastatic regions. Bone scintigraphy images used in this paper had poor resolution which made the evaluation of images more difficult.

T. Apiparakoon et al. [6] proposed a CNN model which is based on feature pyramid network (FPN) with some changes to perform lesion instance segmentation called as MaligNet. At some point, the amount of unlabelled data reaches saturation point after which the model efficiency does not increase much.

T. Altameem et al. [7] used Gray-Level Co-Occurrence Matrix (GLCM) for grey-level feature extraction. This method derives the features from intuitionistic fuzzy rank correlation-based segmented region in terms of texture, shape and intensity. The prediction of bone cancer has to be improved through optimization while classifying the extracted bone features.

In O. Bandyopadhyay et al. [8] connected component analysis (CCA) [10] of the single-pixel image of the bone contour is performed. Deformity of the bone contour and the changed textures are analysed to identify the features to be used for decision making. X-ray images are used for detection of metastatic bone but it has lower sensitivity when compared with WBS.

Y. Pi et al. [9] used deep Convolutional Neural Networks (CNNs) to automatically extract high-level features from the input images. Three different CNN models were explored namely Inception-V3, DenseNet and SENet. Inception-V3 when combined with spatial attention operator gives the best performance with an accuracy of 95%.

A. Shimizu et al. [10] introduced butterfly-type networks (BtrflyNets) along with deep supervision (DSV) for skeleton segmentation. DSV is effective in reducing losses in training data. BtrflyNets is used to segment the skeleton and extract the hot spots of bone metastatic lesions. However, limited amount of training data for osteoarthritis resulted in misclassification of lumber and thoracic vertebrae as hot spots of bone metastatic lesions.

Y. Mohamed et al. [11] proposed algorithm based on the Gamma Correction (GC) after image filtering using local gaussian adaptive filter and median filter for enhancing contrast of bones in bone scan. But this algorithm does not consider enhancing the dark parts and removes some important dark parts of the image.

IX. EXPERIMENTAL RESULTS

Qualitative analysis of enhanced as well as input image provides us with the performance of enhancement as well as change in contrast and brightness of the image. Randomly selected images were evaluated qualitatively and quantitatively (perception-based image quality evaluator (PIQE), Effective Measure of Enhancement (EME), absolute mean brightness error, structural similarity (SSIM), and peak signal to noise ratio (PSNR)) to select a range of gamma values (from 0.1 to 0.9, with increment of 0.1), where the results were acceptable. It was seen that the range of gamma values from 0.4 to 0.7 was found to be optimum. The single gamma value of 0.5 resulted in majority of the images to be acceptable.

$$\text{EME} = \frac{1}{rc}\sum_1^r \sum_1^c \left[20\ln\left(\frac{\text{Imax}}{\text{Imin}}\right)\right] \tag{2}$$

To calculate PSNR, the block first computed the mean-squared error (MSE) using following equation:

$$MSE = \frac{\sum_{M,N}[I_1(m,n) - I_2(m,n)]^2}{M*N} \tag{3}$$

Where M and N are the number of rows and columns in the input images. Then the block calculates PSNR using the following equation:

$$PSNR = 10\log_{10}\left(\frac{R^2}{MSE}\right) \tag{4}$$

Where R is the maximum fluctuation in the input image data type.

TABLE III

Gamma Value	PSNR	SSIM	PIQE
0.4	19.58	0.4126	47.731
0.5	20.67	0.8723	43.7451
0.6	18.81	0.7734	54.2102
0.7	17.02	0.6209	68.0477

Performance evaluation of segmentation gives us the accuracy of segmented ROI. ROI in this project being hotspots are evaluated with the parameters mentioned in TABLE IV to evaluate the correctness of segmentation.

International Journal for Research in Applied Science & Engineering Technology (IJRASET)
ISSN: 2321-9653; IC Value: 45.98; SJ Impact Factor: 7.538
Volume 11 Issue V May 2023- Available at www.ijraset.com

TABLE IV

PARAMETERS	FORMULAE
JC	$\dfrac{A \cap B}{A \cup B}$
DC	$\dfrac{2JC}{1 - JC}$
OR	$\dfrac{DC}{2 - DC}$
HD	$\max[bw(i,j), bw2(j,i)]$

The value of parameters Jaccard Coefficient (JC), Dice Coefficient (DC) and Overlap Ratio (OR) ranges between 0 & 1. These values when reach closer to 1 then it indicates a complete sync with the ground truth hence showing complete segmentation. Whereas smaller the value of HD more successful is the segmentation.

We got JC= 1, DC= 1, OR= 1 for most of the segmented images, which shows a good result of our segmentation technique.

GLCM features are statistical measures extracted from the GLCM matrix.

TABLE V

Features	Value(s)
Correlation	0.9724
Energy	0.6325
Homogeneity	0.9636
Contrast	0.0847

The features learned by the CNN can then be used for classification tasks. The confusion matrix shows the total number of observations in each cell. Rows of the confusion matrix corresponds to the True class whereas columns corresponds to the predicted class. Diagonal & off-diagonal cells represent conform to correctly & incorrectly classified observations respectively.

A confusion matrix is shown in Fig. 10. Based on the confusion matrix provided below, model has made a total of 19 predictions, with 15 True Positives (TP), 0 False Positives (FP), 1 False Negative (FN), and 3 True Negatives (TN).
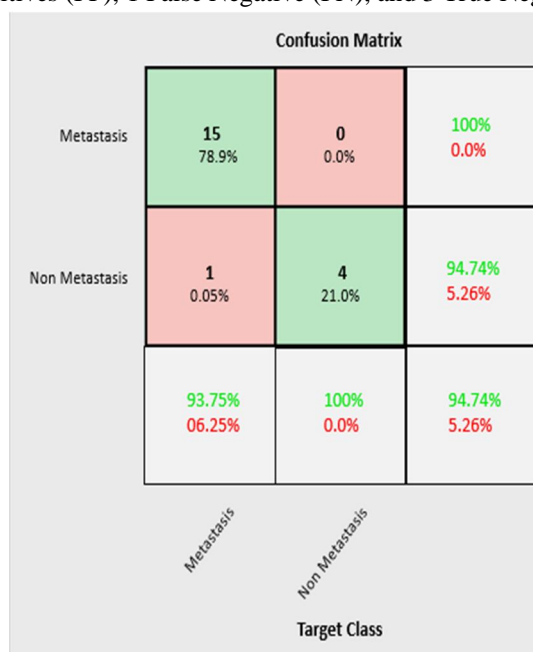

Fig. 10 Confusion Matrix

This confusion matrix is used to define the performance of classification algorithm.

TABLE VI

Parameters	CNN (%)
Sensitivity	93.75
Specificity	100
Accuracy	94.74
Precision	100
Recall	93.75
F1- score	96.77

X. CONCLUSION

Computer-Aided Detection method is used to avoid mistakes occurs due to human interference & experimental sources. CAD system provides simpler and more precise results that facilitates in the early detection of bone metastasis, which increases the patient's chance of survival. The method of segmentation can be improved further to attain region of interest more accurately & precisely as it helps to determine the hot-spot and in classification of images. Optimization in the hyper-parameters of deep neural networks, e.g., number of layers, number of channels (feature maps) and weights in loss functions, is also very crucial in order to boost the performance in terms of extraction accuracy as well as computational cost.

REFERENCES

[1] F.G. Elfarra, M. A. Calin and S. V. Parasca, "Computer-Aided Detection of Bone Metastasis in Bone Scintigraphy Images using Parallelepiped Classification Method," Annals of Nuclear Medicine, Vol. 33, pp. 866-874, September 2019.

[2] M.M. Nasef, F.T. Eid and A.M. Sauber, "Skeletal Scintigraphy Image Enhancement based Neutrosophic Sets and Salp Swarm Algorithm," Journal Artificial Intelligence in Medicine, Vol. 109, pp. 1-10, September 2020.

[3] M. A. Calin, F.G. Elfarra and S. V. Parasca, "Object-oriented Classification Approach for Bone Metastasis Mapping from Whole-Body Bone Scintigraphy," Journal of Physica Medica, Vol. 84, pp. 141-148, April 2021.

[4] A. Sharma, A.K. Pandey, D. Khichi and R. Kumar, "Methylene Diphosphonate Bone Scan Scintigraphic Image Enhancement using Gamma Correction and Optimizing the Value of Gamma," Indian Journal of Nuclear Medicine, Vol. 35, No. 1, pp. 21-27, January 2020.

[5] A. Aslantas, E. Dandil, S. Sağlam and M. Çakiroğlu, "CADBOSS: A Computer-Aided Diagnosis System for Whole-Body Bone Scintigraphy Scans," Journal of Cancer Research and Therapeutics ,Vol. 12, No. 2, pp. 787-792, June 2016.

[6] T. Apiparakoon, N. Rakratchatakul, M. Chantadisai, U. Vutrapongwatana, K. Kingpetch, S. Sirisalipoch, Y. Rakvongthai, T. Chaiwatanarat and E. Chuangsuwanich, "MaligNet: Semisupervised Learning for Bone Lesion Instance Segmentation Using Bone Scintigraphy," IEEE Access, Vol. 8, pp. 27047 – 27066, February 2020.

[7] T. Altameem, "Fuzzy Rank Correlation-Based Segmentation Method and Deep Neural Network for Bone Cancer Identification," Neural Computing and Applications, Vol. 32, pp. 805-815, January 2019.

[8] O. Bandyopadhyay, A. Biswas and B. B. Bhattacharya, "Bone-Cancer Assessment and Destruction Pattern Analysis in Long-Bone X-ray Image," Journal of Digital Imaging, Vol. 32, pp. 300-313, October 2018.

[9] Y. Pi, Z. Zhao, Y. Xiang, Y. Li, H. Cai and Z. Yi, "Automated Diagnosis of Bone Metastasis Based on Multi-View Bone Scans using Attention-Augmented Deep Neural Networks," Journal of Medical Image Analysis, Vol. 65, pp. 1-11, July 2020.

[10] A. Shimizu, H. Wakabayashi, T. Kanamori, A. Saito, K. Nishikawa, H. Daisaki, S. Higashiyama and J. Kawabe, "Automated Measurement of Bone Scan Index from a Whole-Body Bone Scintigram," International Journal of Computer Assisted Radiology and Surgery, Vol. 15, pp. 389-400, December 2019.

[11] Y. Mohamed, Y. Abdallah and E. Wagallah, "Improvement of Bone Scintigraphy Image Using Image Texture Analysis," International Journal of Clinical Medicine Research, Vol. 3, No. 6, pp. 99-104, December 2016.

INTERNATIONAL JOURNAL
FOR RESEARCH

IN APPLIED SCIENCE & ENGINEERING TECHNOLOGY

Call : 08813907089 ⓦ (24*7 Support on Whatsapp)